Accepted Manuscript

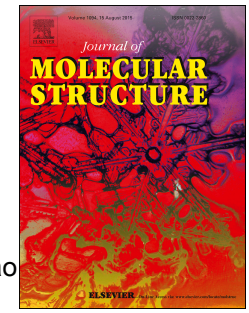

Polymorphism and configurational isomerism in 3-(9-anthryl)-1-(3-hydroxyphenyl)prop-2-en-1-one

Qi Feng, Jiali Wang, Wenhui Huan, Chao Shen, Fang Guo, Jiadan Lu, Guowang Diao

PII: S0022-2860(19)30325-4

DOI: https://doi.org/10.1016/j.molstruc.2019.03.049

Reference: MOLSTR 26318

To appear in: *Journal of Molecular Structure*

Received Date: 12 October 2018

Revised Date: 14 March 2019

Accepted Date: 15 March 2019

Please cite this article as: Q. Feng, J. Wang, W. Huan, C. Shen, F. Guo, J. Lu, G. Diao, Polymorphism and configurational isomerism in 3-(9-anthryl)-1-(3-hydroxyphenyl)prop-2-en-1-one, *Journal of Molecular Structure* (2019), doi: https://doi.org/10.1016/j.molstruc.2019.03.049.

Polymorphism and configurational isomerism in 3-(9-anthryl)-1-(3-hydroxyphenyl)prop-2-en-1-one

Qi Feng,[a] Jiali Wang,[a] Wenhui Huan,[a] Chao Shen,[a] Fang Guo,[a] Jiadan Lu,[a] Guowang Diao*[a]
[a] School of Chemistry & Chemical Engineering, Yangzhou University, Yangzhou, 225002

Abstract

In this study, 3-(9-anthryl)-1-(3-hydroxyphenyl)prop-2-en-1-one was synthesized and formed two *cis* isomers (α and β polymorphs) and one *trans* isomer under different crystallization conditions. Single crystal X-ray diffraction revealed that all the three crystals exhibit the similar crystal structures, in which the two adjacent chalcone molecules form dimers through intermolecular H-bonds between the phenolic hydroxyl and carbonyl groups, and all of the dimers stack parallel to construct their 3D structures. In order to rationalize the configurational phenomenon and investigate the stability of the three crystals, Hirshfeld surface analyses, theoretical calculation and grinding experiments were performed. The results revealed that the coexistence of H-bonds and C-H$\cdot\cdot\pi$ interactions around the two hydrogen atoms on the C=C double bond may be crucial for formation of the *cis* configuration, and the *trans* isomer is more stable than the other two *cis* isomers. Moreover, the optical-physical properties of these crystals were also investigated. Due to the similar crystal structures, the similar fluorescence bands were observed in their spectra.

Keywords: configurational isomerism, chalcone, polymorphism

Introduction

Cis–trans isomerism of organic compounds, also known as geometric isomerism or configurational isomerism, is always a subject of great interest from both academia and industry, for their distinctive physical and chemical properties, such as solubility, stability and mechanical properties (tabletability), *etc* [1-6].

The importance of *cis–trans* isomerism in luminescent material system was also underscored, because the different configuration of a given molecule usually exhibits distinct optical-physical properties [7,8]. For example, 5-(-1-(4-bromo-phenyl)-3*a'*,7*a'*-hexahydro-1*H*-indazol-3-yl)-3-methyl-1-phenyl-1H-pyrazole-4-carbonitrile (PZ) displays an emission band at 396 nm in *trans* form, whereas its fluorescence emission maximum is 475 nm in *cis* form [9].

Chalcone [10], an important natural compounds possessing a wide range of bioactivities [11], can be also used as organic luminescent materials due to their excellent optical-physical properties [12,13]. In this study, an chalcone derivative, 3-(anthracen-9-yl)-1-(3-hydroxyphenyl)prop-2-en-1-one (Scheme 1), was synthesized and some interesting solid state behaviors have been observed. The compound afforded three different crystals from a variety of different solvents. Single crystal X-ray analyses revealed that two of them adopt the *cis* configuration and only one exhibits a *trans* configuration. The *trans* isomer crystallizes in a monoclinic system with space group *C*2/*c*, and its asymmetric units (ASU) accommodates one crystallographically independent molecule. However, both the two *cis* isomers (named as α and β polymorphs) crystallize in the triclinic system with space group $P\bar{1}$, and their ASUs accommodate two and one crystallographically independent molecules, respectively. To the best of our knowledge, for the chalcone derivative, the *trans* isomers usually exhibit greater stability than the *cis* isomers, and many

chalcones in the previous reports, such as 3-(1-pyrenyl)-1-(4-chlorophenyl)prop-2-en-1-one, 1-phenyl-3-(1-pyrenyl)prop-2-en-1-one and 4-bromo-1-naphthyl Chalcone, mainly adopt *trans* configuration due to their strikingly steric effect and stabilities [14,15]. Conformational polymorphism was rarely reported for the *cis* chalcone molecules, even rarer an ASU accommodates two *cis* conformers simultaneously [16]. Based on the three crystal structures, computational methods were performed for rationalizing the configuration phenomenon and investigating their stability. Meanwhile, the solid-state properties of the three crystals were also investigated.

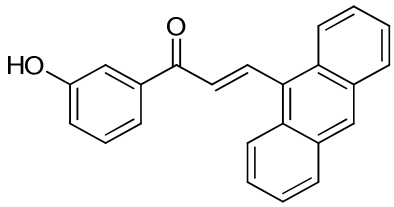

Scheme 1. Chemical structure of 3-(anthracen-9-yl)-1-(3-hydroxyphenyl)prop-2-en-1-one.

Experiment

Material Synthesis and Characterization

The chalcone molecule was synthesized and characterized by a previous reported method [18]. A mixture of 3-hydroxyacetophenone (1.6 g), 9-anthracenecarboxaldehyde (2.3 g), and 3 M of aqueous sodium hydroxide (6 mL) in ethanol (20 mL) was stirred at 50°C for 16 h. The crude product was collected by filtration and recrystallized from 95% ethanol to give pure chalcone (*trans* isomer) as orange crystals: 2.71 g, yield: 74.9%, mp: 198-200 °C. ^{1}H NMR (DMSO, Figure 1S of the Supporting Information): δ (ppm) 7.03−7.08 (dd, 1H), 7.32−7.38 (t, 1H), 7.46−7.49 (t, 1H), 7.53−7.64 (m, 6H), 8.10−8.17 (dd, 2H), 8.21−8.28 (d, 2H), 8.55−8.62 (d, 1H), 8.67 (s, 1H), 9.83(s, 1H). ^{13}C NMR (DMSO, Figure 2S): δ (ppm) 115.13, 120.18, 121.00, 125.44, 126.05, 127.25, 128.70, 129.32, 129.43, 130.14, 130.47, 131.29, 131.85, 139.10, 140.59, 158.23, 189.13.

Crystals' Preparation

The preparation of the *trans* isomer crystals has been mentioned in the synthesis part. *α* polymorph of the *cis* isomers was recrystallized from ethanol/chloroform mixed solvent (v : v = 1 : 3). Slow evaporation of the solvent at room temperature for 4–5 days yielded orange needlelike crystals. However, despite extensive efforts, *β* polymorph of the *cis* isomers was obtained only once from acetone/dichloromethane (v : v = 1 : 1) mixed solvent. Since it was difficult to get an adequate amount of *β* polymorph, only its single crystal data was measured.

Measurement

Single crystal X-ray diffraction experiments were carried out using a Bruker D8 QUEST diffractometer equipped with a Bruker APEX-II (λ = 0.71073 Å). Data collection for the three crystals was done at ambient temperature. Crystal structures were solved with direct methods using SHELXL-2014 program and refined anisotropically using a full-matrix least-squares procedure [19]. All non-hydrogen atoms were refined anisotropically. All the hydrogen atoms, including hydrogen atom of the phenolic hydroxyl groups, were inserted at their calculated positions and fixed at their positions. The structural data for three crystals have been deposited as CIFs at the Cambridge Crystallographic Data Base (CCDC No. 1868346, 1855435 and 1868347) and are also available as Supporting Information (SI). Powder X-ray diffraction (PXRD) patterns were measured with a Bruker D8 advance superspeed powder diffractometer, which operated at ambient temperature, using Cu Kα radiation (λ = 0.15405 nm).

UV-Vis absorption spectra were recorded on a Shimadzu UV-3600 spectrometer. Fluorescence spectra were obtained on a Horiba FluoroMax 4 spectrofluorometer. Quantum yields of the chalcone in different solvents were also determined on Horiba FluoroMax 4 spectrofluorometer, quinolone sulfate in 0.5 M H_2SO_4 was used as a

standard and excitation was chosen at 365 nm. Solid fluorescent quantum yields were obtained by using an Edinburgh Instrument with an excitation wavelength at 365 nm.

Hirshfeld surface analysis

Hirshfeld surface graphical representation over d_{norm} around each crystallographically independent molecule in the three polymorphs, and associated 2D fingerprint plots were performed out by using Crystal Explorer 3.1 [20].

Calculation Details

Comparison of crystals' stability

The geometry optimization of crystals was performed starting from the X-ray structures. Cambridge Sequential Total Energy Package (CASTEP) module based on the Planewaves Pseudopotential method of density functional theory (DFT) was used to optimize three crystals, and the most stable structures and energy are calculated. Generalized Gradient Approximation (GGA) and Perdew-Burke-Ernzerhof (PBE) exchange-correlation functional were used. To ensure the correctness of the calculation, the cut-off energy was selected as 400.0 eV. All the calculations were performed by Material Studio 6.0 program [21].

Theoretical study of spectra

Structural, electronic and optical properties were studied in the framework of the density functional theory (DFT). The M062X functional with 6-31+G (d,p) basis set level was chosen to calculate excited state [22]. All calculations were performed using the Gaussian 09 version B.01 suite of programs [23]. The absence of imaginary frequency modes for the optimized structures at the DFT level confirms a true minimum on the potential energy surface. Further analyses of electronic and optical properties were performed by calculations of both vertical and adiabatic ionization potentials and the calculation of the visible-UV absorption and emission spectra in the framework of time-dependent DFT (TD-DFT).

Result and Discussion

Crystal structure

Single crystal X-ray diffraction analyses were performed for the three crystals to determine their structures. Thermal ellipsoids of the chalcone molecules in the three ASUs were shown in Figure 1. It was worth noting that all the *cis* isomers exhibit the similar conformation with each other, in which the dihedral angles between the anthracene and benzene rings are 80.07° (type A in α polymorph), 83.08° (type B in α polymorph) and 82.43° (β polymorph), respectively (Figure 2). In contrast, the *trans* isomer shows a nearly planar structure with the dihedral angle of 29.95°. The crystallographic data was presented in Table 1.

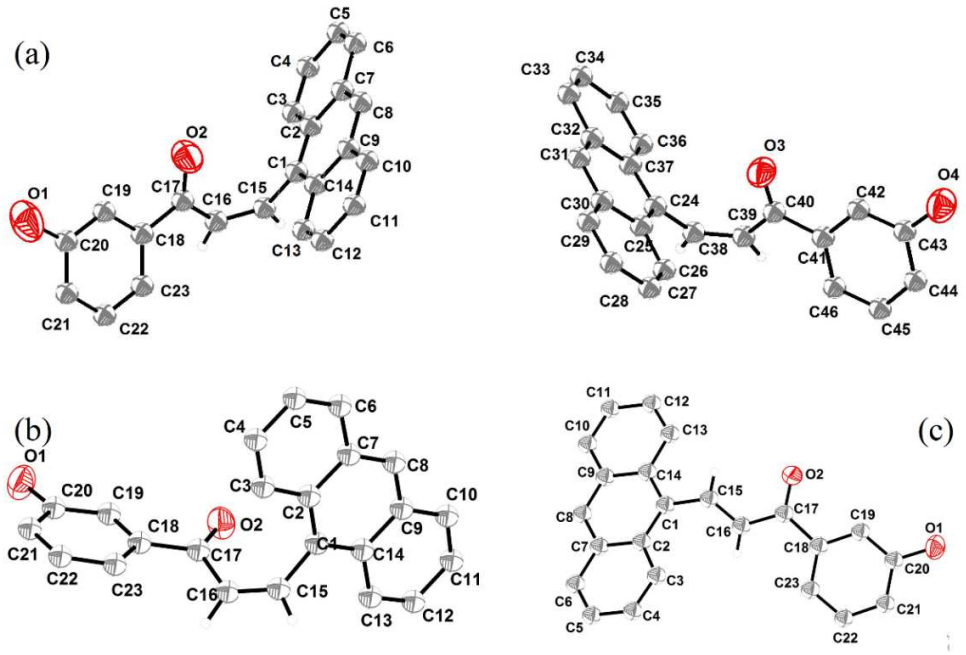

Figure 1. Thermal ellipsoids plots of the two *cis* isomers (a and b) and *trans* isomer (c).

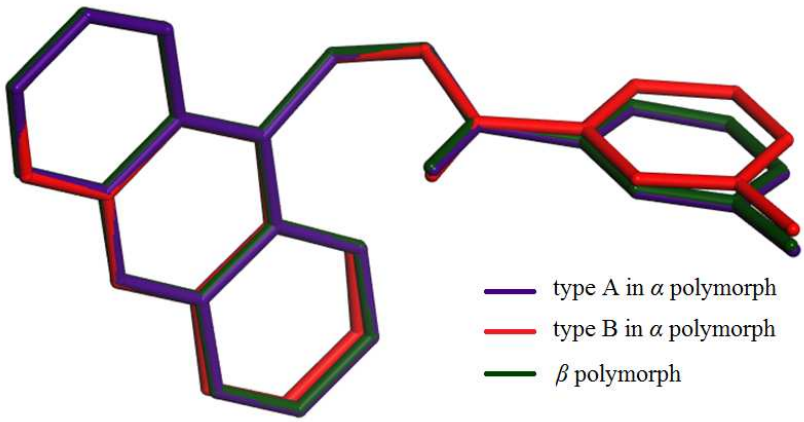

Figure 2. Comparison of the conformation for the three *cis* isomers.

Table 1. Numerical details of the solutions and refinements of the three crystal structures.

Crystals	*α* polymorph	*β* polymorph	*trans* isomer
Formula	$C_{23}H_{16}O_2$	$C_{23}H_{16}O_2$	$C_{23}H_{16}O_2$
Morphology	needle	needle	needle
Crystal system	triclinic	triclinic	monoclinic
Space group	*P*$\bar{1}$	*P*$\bar{1}$	*C*2/*c*
a / Å	5.4651(6)	5.4587(6)	33.809(4)
b / Å	16.891(2)	11.5366(14)	5.5199(7)
c / Å	19.743(3)	13.5526(16)	21.394(2)
α /deg	68.888(4)	96.297(4)	90
β /deg	89.737(4)	96.784(4)	124.694(2)

γ /deg	89.614(4)	90.865(4)	90
V/ Å^3	1700.2(4)	842.04(17)	3282.8(7)
Z	4	2	8
ρ (calcd)/Mg m^{-3}	1.267	1.279	1.313
θ Range for data collection/°	2.418–27.581	1.523–27.576	2.316–27.548
F(000)	680	340	1360
R_1, w R_2 ($I > 2\sigma(I)$)	0.0577, 0.1132	0.0571, 0.1464	0.0601, 0.1490
R_1, w R_2 (all data)	0.1735, 0.1424	0.1211, 0.1794	0.1057, 0.1679
Goodness-of-fit	1.002	1.098	1.068
CCDC	1868346	1855435	1868347

It was interesting that the three crystals have the similar structures. As shown in Figures 3−5, due to the intermolecular H-bonds (O-H···O, summarized in Table 2) between the phenolic hydroxyl and carbonyl groups, the chalcone molecules in all the three crystals pair up and generate the molecular dimers. In the *β* polymorph and *trans* isomer, the molecular dimers are parallel stacked along the *a*, *b* and *c* axes to give their 3D structures. The analogous structure could be found in the monoclinic polymorph of 1-phenyl-3-(3-hydroxyphenyl)-2-propen-1-one, where the molecular dimer constructed *via* H-bonds (O-H···O) is also the repeating motif [24] Compared with above two crystals, the *α* polymorph possesses two types of chalcone molecules, namely types A and B. In this crystal, the two adjacent chalcone molecules connect with each other and form A-A or B-B dimers. These dimers are stacked alternately along the *c* axis and adopt parallel arrangement along the *a* and *b* axes to provide its 3D structure. Furthermore, in the three crystals, the closest centroid distances between the anthracene rings is 5.459 Å, thus no strong π-overlap exist among them.

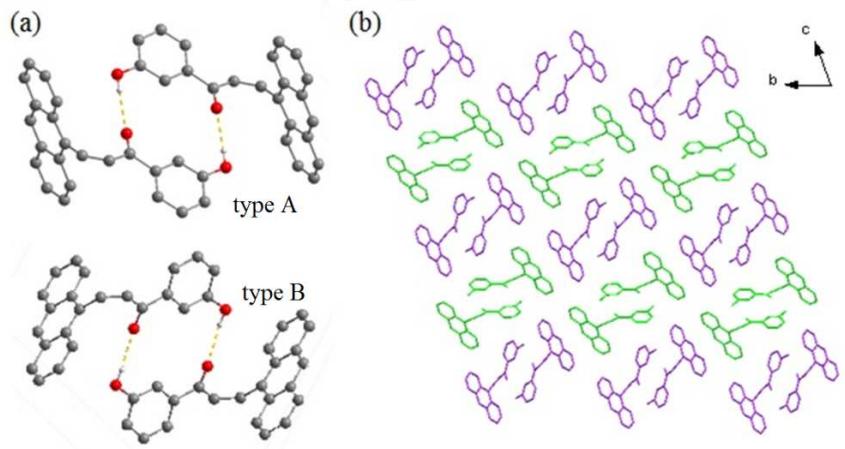

Figure 3. Crystal structure of *α* polymorph. (a) The two types of the hydrogen bonding dimers. (b) 3D packing diagram of *α* polymorph projected in the *bc* plane. The types of A and B chalcone molecules are shown in purple and green, respectively. Hydrogen atoms not participating in the interactions have been omitted for clarity.

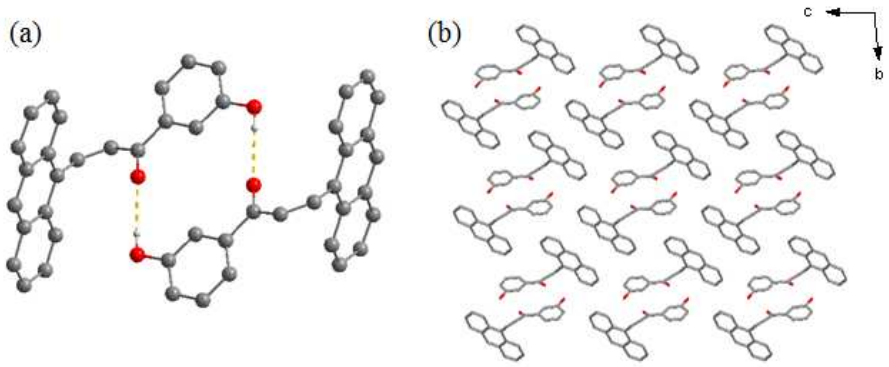

Figure 4. Crystal structure of *β* polymorph. (a) The hydrogen bonding dimer. (b) 3D packing diagram of *β* polymorph projected in the *bc* plane. Hydrogen atoms not participating in the interactions have been omitted for clarity.

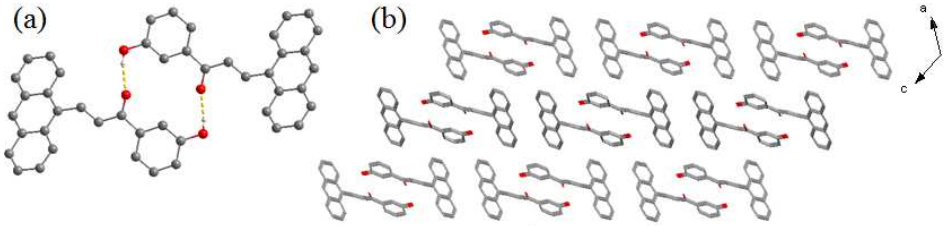

Figure 5. Crystal structure of the *trans* isomer. (a) The hydrogen bonding dimer. (b) 3D packing diagram of the *trans* isomer projected in the *ac* plane. Hydrogen atoms not participating in the interactions have been omitted for clarity.

Table 2. H-bonds geometry (Å, deg) in the three crystals.

Crystals	D-X···A	D-X	X···A	D···A	D-X···A
α polymorph	O1–H16···O2	0.82	2.14	2.916(2)	159.2
	O4–H32···O3	0.82	2.09	2.900(2)	169.3
β polymorph	O1–H16···O2	0.82	2.10	2.8973(19)	163.3
trans isomer	O1–H1···O2	0.82	2.07	2.8637(18)	162.0

Powder X-ray Diffraction (PXRD) Patterns and FT-IR Spectroscopy

As shown in Figure 6, PXRD patterns of *α* polymorph and *trans* isomer are distinctly different and are in agreement with that simulated from their crystal data. Thus, the powder product could be used for the solid-state properties investigation later.

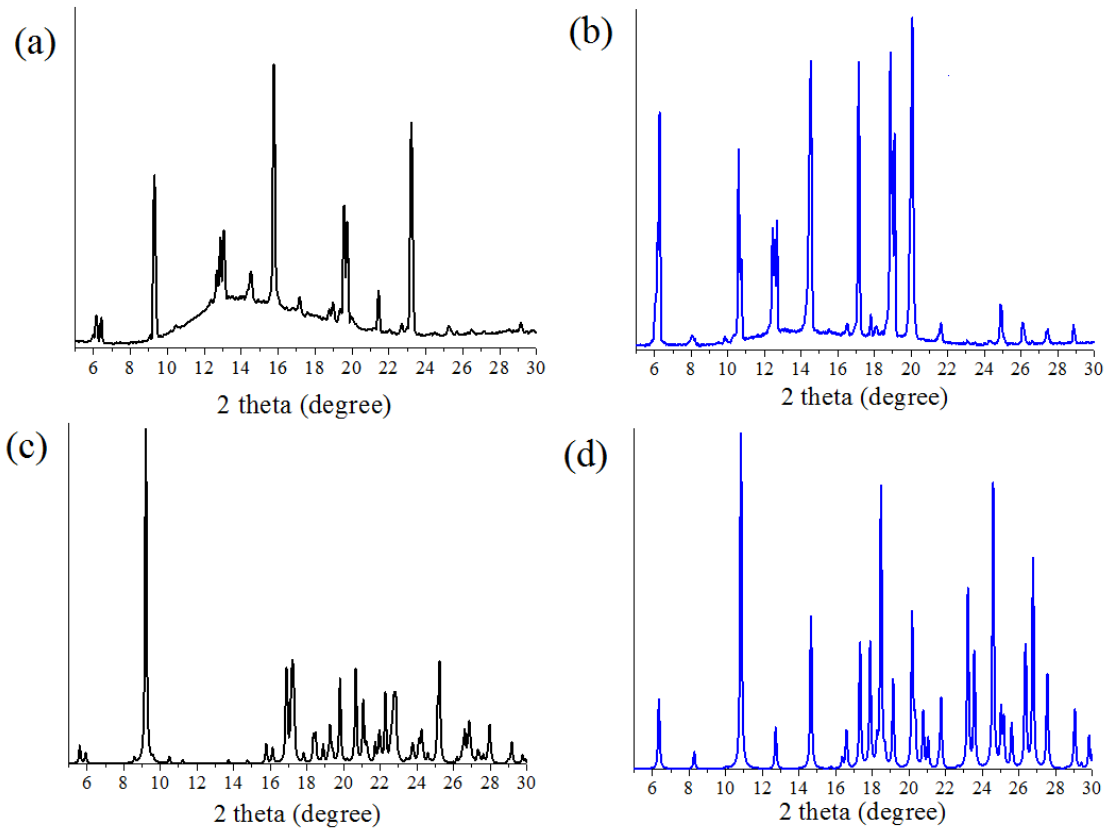

Figure 6. Comparison of the experimental and simulated PXRD patterns of the *α* polymorph (a and c) and *trans* isomer (b and d).

FT-IR spectra were also recorded to identify the *cis* and *trans* isomers. From the fingerprint spectra, the two peaks with medium intensity at 773 and 993 cm^{-1} could be observed in their fingerprint areas (Figure 7a, the entire spectra were shown in Figure 3S), corresponding to the two peaks at 793 and 1039 cm^{-1}, which were calculated in ideal gas phase conditions (Figure 7b). The two peaks are specific for the nonplanar deformation vibrations of the hydrogens of an ethylenic bond in the *cis* or *trans* isomer, suggesting that the opposite configuration between the two crystals.

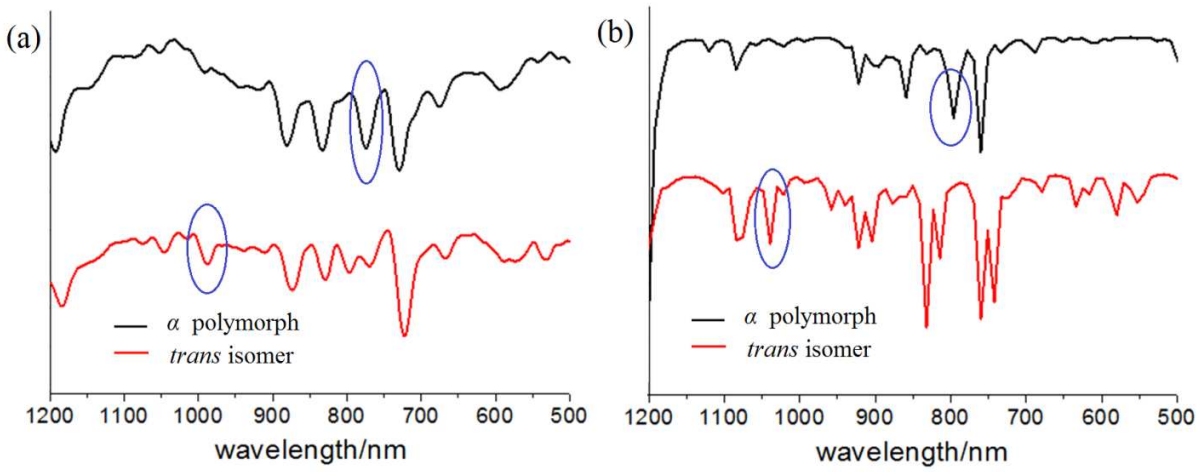

Figure 7. The experimental and simulated fingerprint spectra of *α* polymorph (a) and *trans* isomer (b).

Configuration and stability analyses of 3-(9-anthryl)-1-(3-hydroxyphenyl)prop-2-en-1-one

In contrast to many other chalcone molecules exhibiting the *trans* configuration, the chalcone in this study mainly exhibits the *cis* configuration. Aiming to rationalize the configurational phenomenon of this chalcone, computational methods were performed.

First, Hirshfeld surface was performed to give insights regarding the important intermolecular interactions in the three crystals. The inspection of the intermolecular interactions was normalized by van der Waals radii through a red-white-blue color scheme, where the red spots denote closer contacts of molecules. The non-covalent interactions occurring within the structures have clear signatures on the fingerprint plots.

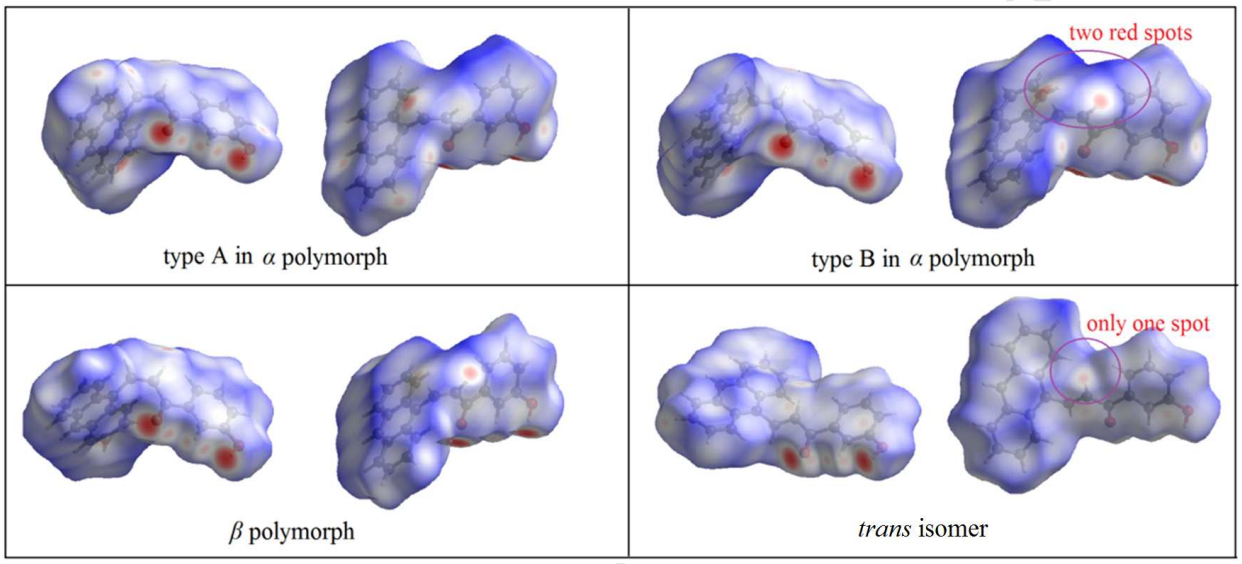

Figure 8. Hirshfeld surface mapped with d_{norm} for the four independent molecules in the three crystals.

From the Hirshfeld surface (Figure 8), it was obviously observed that all the four chalcone molecules exhibit two red spots on the phenolic hydroxyl and carbonyl groups, corresponding to the H-bonds (O-H···O) for constructing the molecular dimers. That is to say, these H-bonds play a key role in crystal packing for the three crystals. In addition, for each molecule in *α* and *β* polymorphs, another two red spots could be found around the hydrogen atoms on C=C double bond (one red spot on type A molecule in *α* polymorph is not very obvious), which should be ascribed to the interactions among the 1D chain motifs in crystal structures (Table 3). Take type A molecule for example (Figure 9), one spot should be assigned to the weak H-bond (C=O···H) associated with carbonyl group from the neighboring chalcone molecule, another spot could be assigned to intermolecular C-H···π interaction. However, for the *trans* chalcone, only one red spot corresponding to the intermolecular H-bond (C=O···H) was observed around C=C double bond. Based on the Hirshfeld surface analyses, a conclusion could be drawn that the coexistence of H-bond (C=O···H) and C-H···π interactions around C=C double bond are crucial for formation of the *cis* isomer, which like two hands pull the two hydrogen atoms to the same side of C=C double bond. In contrast, disappearance of one interaction would result in formation of the *trans* chalcone configuration.

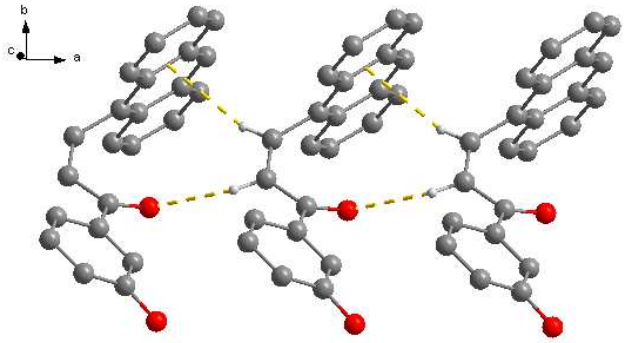

Figure 9. H-bond (C=O···H) and C-H··π interaction around the hydrogen atoms on C=C double bond.

Table 3. Weak H-bonds and C-H··π interactions geometry (Å, deg) in the three crystals.

Crystals	D-X···A	D-X	X···A	D···A	D-X···A
α polymorph	C16–H11···O2	0.930	2.670	3.434	139.91
	C15–H10··π	0.819	2.673	3.566	161.20
	C39–H27···O3	0.930	2.517	3.353	149.67
	C38–H26··π	0.929	2.877	3.802	173.34
β polymorph	C16–H11···O2	0.971	2.465	3.331	148.50
	C15–H10··π	0.930	2.857	3.766	166.22
trans isomer	C16–H16···O2	0.930	2.608	3.486	157.78

Table 4 summarized the contacts contributing to the Hirshfeld surface represented in normal mode. It was found that weak H···H contacts display the major contributionin all the three polymorphs, with 44.2%, 41.9%, 43.8% and 43.0% of total surface area, respectively. The C···H contacts with second major contribution comprise 38.2%, 40.1%, 38.2% and 37.1% of total surface area. Apart from that, O···H contacts in the three polymorphs also show important contribution for the supramolecular architectures from 12.3 to 14.6% of total surface area and appear as two wings in the left (H···O) and right (O···H) areas of the related plots (Figure 10).

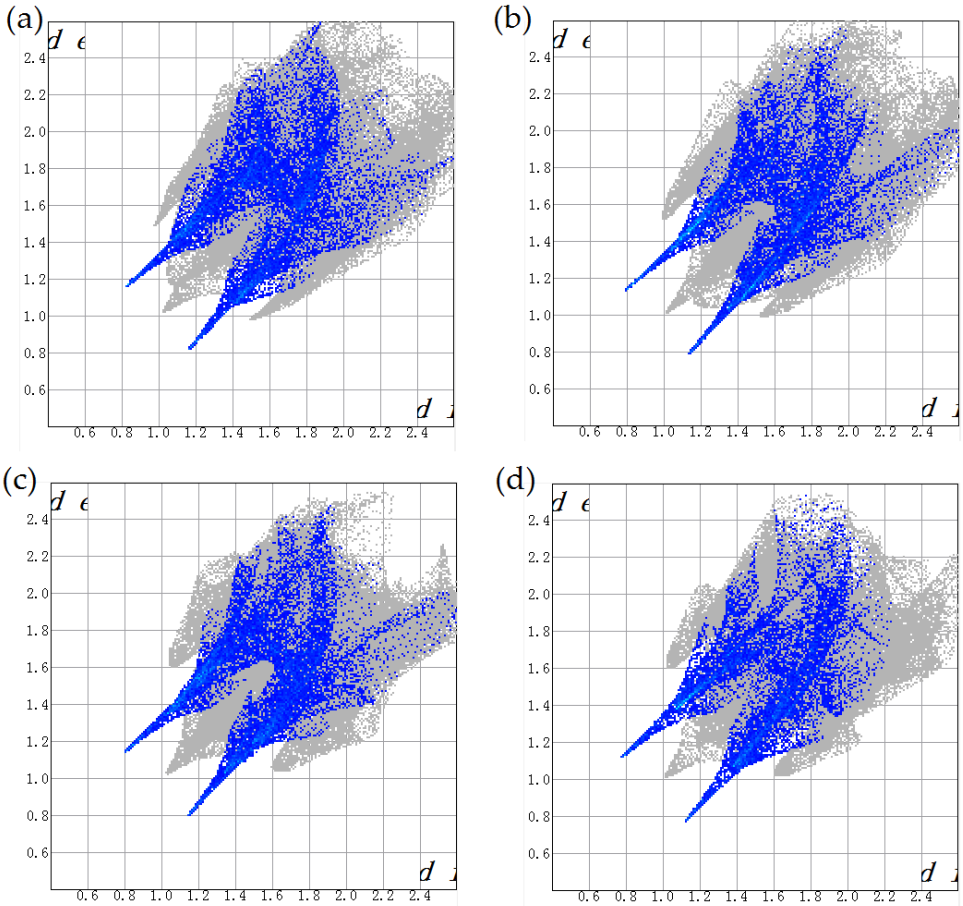

Figure 10. Two-dimensional fingerprint plots for O···H / H···O contacts: types A (a) and B (b) in *α* polymorph, *β* polymorph (c) and *trans* isomer (d).

Table 4. Contributions of the intermolecular contacts.

Chalcone molecule	H···H %	C···H %	O···H %	C···C %	C···O %
α polymorph (type A)	44.2	38.2	14.3	2.3	1.1
α polymorph (type B)	41.9	40.1	14.6	1.8	1.7
β polymorph	43.8	38.2	14.3	2.5	1.3
trans isomer	43.0	37.1	12.3	5.2	2.4

Second, according to former research, the most chalcone molecules contained large π-conjugated groups, such as anthryl or pyrenyl, usually exhibit twisted structure [25,26]. However, in our system, the dihedral angles between the anthracene and benzene rings in all the *cis* isomers are nearly vertical. In contrast, the *trans* chalcone molecule shows a nearly planar structure. In order to investigate stability of the three crystals, theoretical calculation and correlative phase transition experiments were performed.

Calculation details has been described in experiment part. Fixed the unit cell parameters, the molecules were relaxed to obtain the energy of each unit cell, and the result was summarized in Table 5. It could be found that the *trans* isomer exhibits lowest energy of 4690.19 eV, which has 0.18 and 0.1eV lower than *α* and *β* polymorphs, suggesting it is more stable than the other two *cis* polymorphs. Moreover, as shown in Figure 11, the conversion energy barrier from *cis* isomer to *trans* isomer was also calculated by DFT in gas phase condition at M062X/6-31+G(d,p) level. The *cis* isomer need to overcome 181.453 kcal/mol for transforming into *trans* isomer.

In order to verify the above result, the phase transitions were investigated. Analysis of the grinding product by PXRD patterns (Figure 5S), whether or not the solvent was added, the α polymorph always transformed into the *trans* ismoer polymorph. This result further proved that the *trans* isomer is more stable, which may be also responsible for unavailability of β polymorph, despite extensive efforts.

Table 5. The energy (eV) of the three polymorphs calculated by GGA-PBE method (cut-off energy 400.0 eV) [27].

Optimized crystal structure[a]	energy
α polymorph	-4690.01
β polymorph	-4690.09
trans isomer	-4690.19

[a] Optimized super cell were shown in Figure 4S.

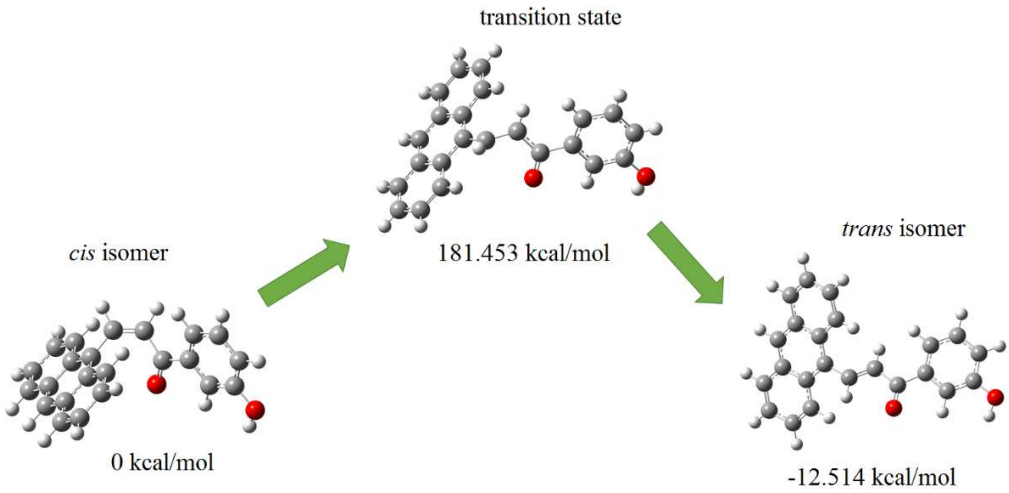

Figure 11. Conversion energy barrier from *cis* isomer to *trans* isomer.

Optical–physical properties

The absorption and fluorescence spectra of the chalcone in various solvents with different polarities were shown in Figure 12. The absorption spectra show very little change with an increase in the solvent polarity and exhibit the narrow absorption bands with the absorption maxima around 250 nm. Besides, several weak absorption bands in 340–420 nm could be also observed, which are attributed to anthracene chromophore [28]. Agreeing with the above experiments, TD-DFT calculation revealed that the chalcone molecule (*trans* isomer) has two dominant absorption bands (Figure 13a). The one band was found at 5.10 eV (243 nm), which is associated with HOMO-2→LUMO transition. The other band is around 3.24 eV (383 nm), corresponding to HOMO→LUMO transition.

In Figure 12b, the fluorescence spectra in various solvents were presented. Compared with the absorption spectra, the intensity of fluorescence peaks exhibits obvious change with an increase in the polarity of solvents. When the solvent was changed from chloroform to acetonitrile, fluorescence intensity decrease / increase could be found around 280–330 and 360–460 nm in the spectra, respectively. The spectrum of the chalcone in acetonitrile shows vibration peaks at 393, 415 and 438 nm, corresponding to anthracene chromophore emission [28]. However, when measured in the other solvents, the vibration structure is less clear, even disappears almost completely in ethanol.

The emission spectrum of the chalcone molecule (*trans* isomer) in gas phase calculated at the M062X/6-31+G(d,p) level of theory were plotted with respect to the integrated amplitude and were shown Figure 13b. It could be observed that the dominant emission bands are centered at 3.10 eV (404 nm) and 4.03 eV(308 nm), which are attributed to the LUMO→HOMO and LUMO+2→HOMO transitions, respectively.

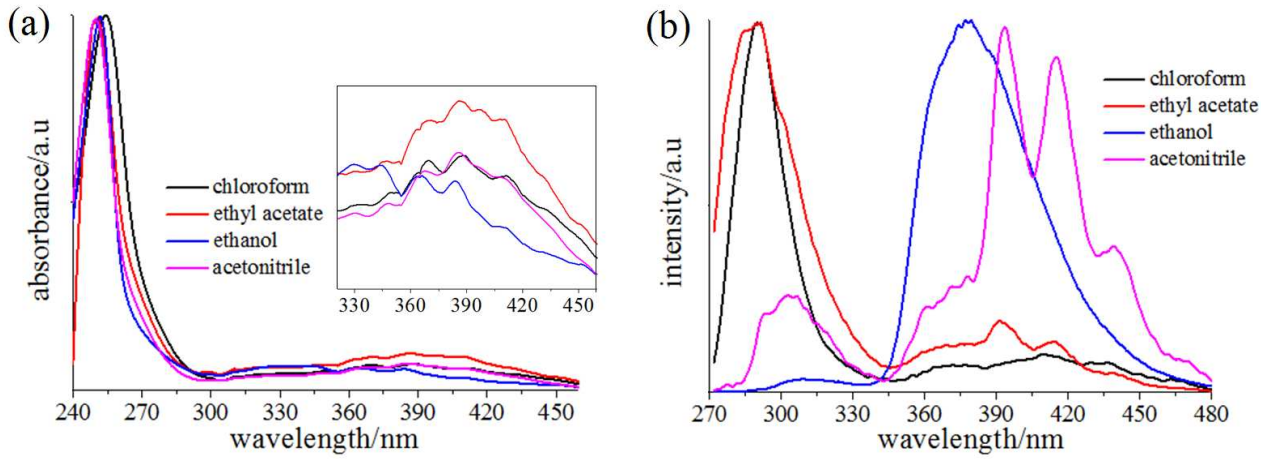

Figure 12. UV-Vis (a) and fluorescence (b) spectra of the chalcone in various solvents.

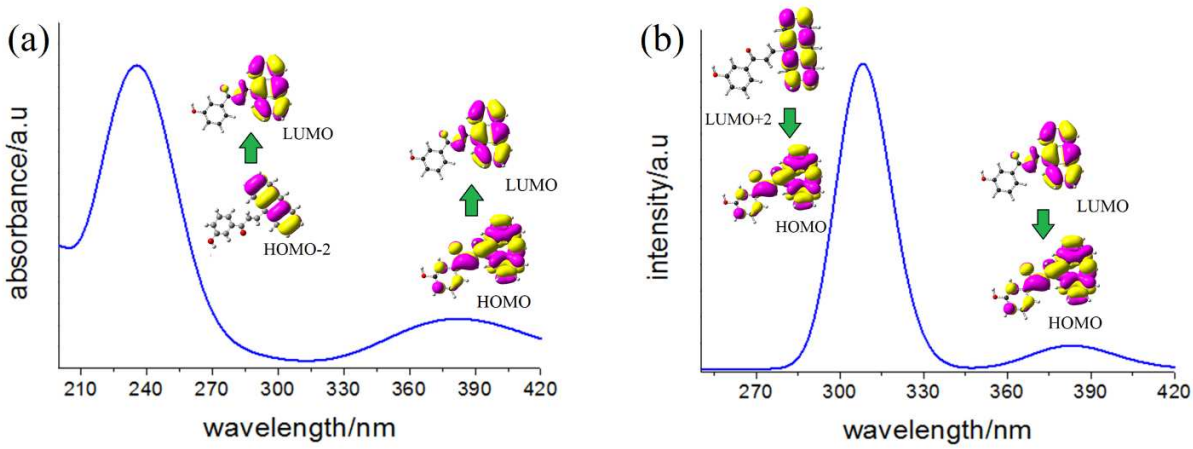

Figure 13. UV-Vis (a) and fluorescence (b) spectra of the chalcone calculated in gas phase at M062X/6-31+G(d, p).

Apart from that, the optical-physical properties of *α* polymorph and *trans* isomer were also investigated. As shown in Figure 14, the *α* polymorph and *trans* isomer have similar absorption spectra, which exhibit a two broad absorption bands around 245 and 300 nm, respectively. Compared with that measured in solvents, the absorption bands in 340–420 nm range almost disappear.

Excited at 365 nm, the weak fluorescence could be observed in both the *α* polymorph and *trans* isomer in our system, they exhibit a broad band with only one peak centered at 592 and 586 nm, respectively. Compared with that measured in solvents, the solid-state emission maxima shift to the longer wavelength region with a red shift of about 160 nm. The solid-state properties of a given molecule are usually closely related to its arrangement. Thus, the similar optical-physical properties of the two crystals should be ascribed to their similar crystal structures.

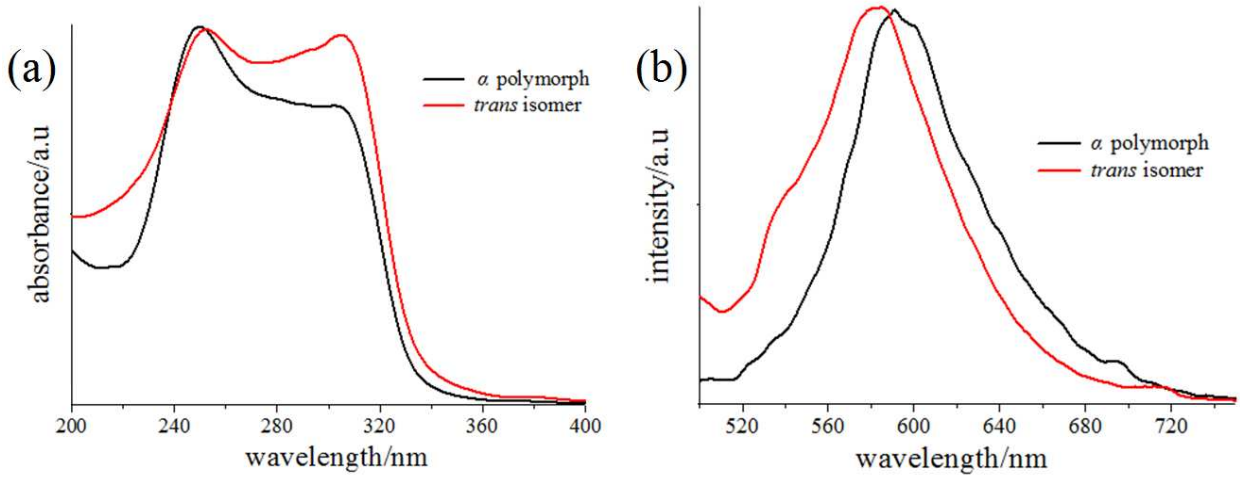

Figure 14. Absorption (a) and fluorescence (b) spectra of the *α* polymorph and *trans* isomer.

Table 6. Optical-Physical Properties Data.

solvents / crystals	λ_{ab} (nm)[a]	λ_{em} (nm)[b]	Φ_F[c]
ethanol	252	377	0.003
chloroform	254	291	0.002
ethyl acetate	251	292	0.002
acetonitrile	250	394	0.001
α polymorph	249	592	0.003
trans isomer	309	586	0.002

[a] Maximum wavelengths of absorption spectra. [b] Wavelengths of fluorescence emission spectra excited at 365 nm for the chalcone in solvents or crystals. [c] Fluorescent quantum yields excited at 365 nm.

Conclusions

In summary, we discovered an interesting polymorphism in 3-(9-anthryl)-1-(3-hydroxyphenyl)prop-2-en-1-one.The compound formed three crystals, two of them adopt the *cis* configuration and only one exhibits the *trans* configuration. All the three crystals exhibit the similar structures, in which the two adjacent chalcone molecules form the dimers and stack parallel to construct their crystal structures. Hirshfeld surface analyses revealed that the intermolecular H-bonds (O-H···O) between the phenolc hydroxyl and carbonyl groups play a key role in crystal packing for the three crystals. However, the coexistence of H-bonds (C=O···H) and C-H··π interactions around C=C double bond are crucial for formation of the *cis* configuration. Moreover, the theoretical calculation and grinding experiments revealed that the *trans* isomer is more stable than the two other *cis* isomers. The optical-physical properties of the *α* polymorph and *trans* isomer were also investigated. Due to their similar crystal structures, no obvious change could be found in their fluorescence spectra.

Conflicts of interest

There are no conflicts to declare.

Acknowledgements

This work is partly supported by the National Natural Science Foundation of China (Grant No. 21773203), Certificate of China Postdoctoral Science Foundation Grant (No. 2018M632387), the Natural Science Foundation of the Jiangsu Higher Education Institutions of China (No. 18KJB150035), and Innovation and Cultivation Fund of Yangzhou University (No. 2017CXJ012).

Notes and references

1 Zhao, Y.; Shen, X. F.; He, S. L; Han, X. G.; Ni, Z. H. *SYNTHETIC MET.* 2018, 245, 175–1181.
2 Dey, D.; Chopra, D. *CrtstEngComm.* 2015, **17**, 5288–5298.
3 Swapna, B.; Suresh, K.; Nangia, A. *Chem.Commun.* 2016, **52**, 4037–4040.
4 Hodges, J. M.; Schaak, R. E. *Accounts Chem. Res.* 2017, **50**, 1433–1440.
5 Klein, C.; Fischer, C.; Seichter, W.; Schwarzer, A.; Weber, E. *CrtstEngComm.* 2011, **13**, 1931–1938.
6 Couzijn, EPA.; Schakel, M; de Kanter, FJJ; Ehlers, AW; Lutz, M; Spek, AL; Lammertsma, K. *Angew. Chem. Int. Edit.* 2004, **43**, 3440–3442.
7 Geng, J.; Tao, T.; Chen, H. Q.; Huang, W. *Inorg. Chem. Commun.* 2014, **42**, 23–28.
8 Li, J. T.; Luo, X. L.; Zhou, Y.; Zhang, L. R.; Huo, Q. S.; Liu, Y. L. *Cryst. Grow. Des.* 2018, **18**, 1857–1863.
9 Mati, S. S.; Sarkar, S.; Sarkar, P.; Bhattacharya, S. C. *J. Phys. Chem. A.* 2012, **116**, 10371–10382.
10 Go, M. L.; Wu, X.; Liu, L. X. *Curr. Med. Chem.* 2005, **12**, 483–499.
11 Labib, M. B.; Sharkawi, S. M. Z.; El-Daly, M. *Bioorg. Chem.* 2018, **80**, 70–80.
12 Cheng, X.; Wang, Z. Y.; Tang, B. L.; Zhang, H. Y.; Qin, A. J.; Sun, J. Z.; Tang, B. Z. *Adv. Funct. Mater.* 2018, **28**, 1706506.
13 Karuppusamy, A.; Vandana, T.; Kannan, P. *J. Photoch. Photobio. A.* 2017, **345**, 11–20.
14 Zhang, R. M.; Wang, M. L.; Sun, H.; Khan, A.; Usman, R.; Wang, S. Z.; Gu, X. T.; Wang J.; Chun, C. X. *New J. Chem.* 2016, **44**, 6441–6450.
15 Nithya, R.; Santhanamoorthi, N.; Kolandaivel P.; Senthilkumar, K. *J. Phys. Chem. A.* 2011, **115**, 6594–6602.
16 Ramos, R. R.; da Silva, C. C.; Guimaraes, F. F.; Martins, F. T. *CrtstEngComm.* 2016, **18**, 2144–2154.
17 James, J. P.; Bhat, K. I.; More, U. A.; Joshi, S. D. *Med. Chem. Res.* 2018, **27**, 546–559.
18 Sheldrick, G. M. *Acta Crystallogr.* 2015, **C71**, 3.
19 Wolff, S. K.; Grimwood D. J.; McKinnon J. J.; Jayatilaka D.; Spackman M. A. CrystalExplorer 3.1, The University of Western Australia, Perth, Australia, 2012.
20 Rajan, R.; Ravindran, T. R.; Venkatesan, V.; Srihari, V.; Pandey, K. K.; Chandra, S.; Mishra, K. K.; Vargeese, A. A. *J. Phys. Chem. A.* 2018, **122**, 6236–6242.
21 Jennings, G.; Smith, M. D.; Kuang, S. M.; Hodges, L. M.; Tyrell, J.; Williamson, R. T.; Seaton, P. *J. Chem. Crystallogr.* 2012, **42**, 159–164.
22 Pandeti, S.; Feketeova, L.; Reddy, T. J.; Abdoul-Carime, H.; Farizon, B.; Farizon, M.; Mark, T. D. *J. Chem. Phys.* 2019, **150**, 014302.
23 Koraiem, A. I.; El-Shafei, A.; Abdellah, I. M.; Abdel-Latif, F. F.; Abd El-Aal, R. M. *J. Mol. Struct.* 2018, **1173**, 406–416.
24 McKinnon, J. J.; Spackman, M. A.; Mitchell, A. S. *Acta Crystallogr.* 2004, **B60**, 627–668.
25 Yu, F. F.; Wang, M. L.; Sun, H.; Shan, Y. Q.; Du, M.; Khan, A.; Usman, R.; Zhang, W.; Shan, H. B.; Xu, C. X. *RSC Adv.* 2017, **7**, 8491-8503.
26 Zhang, R. M.; Wang, M. L.; Sun, H.; Khan, A.; Usman, R.; Wang, S. Z.; Gu, X. T.; Wang J.; Chun, C. X. *New J. Chem.* 2016, **44**, 6441–6450.
27 Nisar, J.; Arhammar, C.; Jamstorp, E.; Ahuja, R. *Phys. Rev. B.* 2011, **84**, 075120.
28 Hanulia, T.; Inami, W.; Ono, A.; Kawata, Y. *Opt. Commun.* 2018, **427**, 266–270.

Dear Referees:

We would like to submit the manuscript entitled “Polymorphism and configurational isomerism in 3-(9-anthryl)-1-(3-hydroxyphenyl)prop-2-en-1-one” to be published in Journal of Molecular Structure. Chalcone have been studied extensively, however, the most chalcone molecules exhibit the *trans* configuration. In this work, an chalcone, 3-(anthracen-9-yl)-1-(3-hydroxyphenyl)prop-2-en-1-one, was synthesized, which afforded three polymorphs under different solvents. To our surprise, two of the three polymorphs exhibit the *cis* configuration, whereas only one exhibit the trans configuration. Hirshfeld surface analyses and theoretical calculation were performed for rationalizing the configuration polymorphism phenomenon and investigating the stability of these crystals. The results revealed that the coexistence of H-bonds and C-H$\cdot\cdot\pi$ interactions around the two hydrogen atoms on the C=C double bond may be crucial for formation of the *cis* configuration, and the *trans* polymorph is more stable than the two other *cis* polymorphs. Meanwhile, several solid-state properties were also investigated. We believed that the study could provide reference for controlling the polymorphism and configuration in chalcone derivatives. We also deeply appreciate your consideration of our manuscript, and look forward to receiving comments from the reviewers. If you have any queries, please don’t hesitate to contact us at the address below.

Thank you and best regards.

Yours sincerely,

Corresponding author:

Name: Guowang Diao

E-mail: gwdiao@yzu.edu.cn